Dissociative Photoionization of Methyl Thiocyanate, CH_3SCN, in the Proximity of the Sulfur 2p Edge

Emiliano Cortés,[†] Mauricio F. Erben,[†] Mariana Geronés,[†] Rosana M. Romano,[†] and Carlos O. Della Védova*[,†,‡]

CEQUINOR (UNLP-CONICET, CCT La Plata), Departamento de Química, Facultad de Ciencias Exactas, Universidad Nacional de La Plata, CC 962, La Plata (CP 1900), República Argentina and Laboratorio de Servicios a la Industria y al Sistema Científico (LaSeISiC) (UNLP-CIC-CONICET), Camino Centenario e/505 y 508, (1903) Gonnet, República Argentina

Received: August 13, 2008; Revised Manuscript Received: November 12, 2008

The dissociative photoionization of gaseous CH_3SCN has been investigated at the S 2p core level using time-of-flight mass spectrometry and synchrotron radiation. The total ion yield spectrum could be successfully assigned by comparison with available data from electron energy loss spectra. The relative abundances of the ionic fragments and their kinetic energy release values were obtained from both PEPICO (photoelectron photoion coincidence) and PEPIPICO (photoelectron photoion photoion coincidence) spectra. The dynamics of the ionic fragmentation of S 2p excited CH_3SCN is dominated by the rupture of both carbon−sulfur bonds. This process may be related with electronic excitations from the ground electronic state to vacant σ^* molecular orbitals.

Introduction

Organosulfur compounds have attracted much attention, and several outstanding reviews covering the chemistry of thiocyanates (RSCN) and isothiocyanates (RNCS) can be found in the chemical literature.[1−3] Simple alkylated species (R = alkyl) are very well-known molecules. For example, methyl isothiocyanate, CH_3NCS, is widely used as an agricultural fumigant, and much attention in recent years has been devoted to understanding the effect of this application on the atmospheric balance.[4] Much information is available for both methyl isomers in their fundamental, ionic, and excited electronic states, and the $CH_3SCN \leftrightarrow CH_3NCS$ isomerization equilibrium has been studied in depth.[2,3]

The molecular structure of isothiocyanate (CH_3SCN) has been determined experimentally using microwave spectroscopy,[5,6] and high-level quantum chemical calculations, including CCSD[7] and QCISD[8] methods, are available for this species. In addition, its vibrational properties have been studied,[9] and infrared spectra in several common solvation environments have recently been reported.[10]

The plasma chemistry of transient species in methyl thiocyanate discharges has been semiquantitatively studied using spectroscopic techniques.[11] The behavior of both isomers, often having been irradiated with VUV synchrotron photons, is quite similar as determined from emission spectra of the NCS radical.[12] In addition, the emission spectra of the radical NCS produced by low-energy electron impact on both isomers have been measured.[13] These studies have been further complemented by laser-induced fluorescence spectroscopy, which succeeded in evaluating the photodissociation process using both 248 and 193 nm wavelengths.[14,15] The gas-phase ion chemistry of CH_3NCS and CH_3SCN has been investigated by pulsed ICR techniques, and their proton affinities are known to be 193.0 ± 0.4 and 192.6 ± 0.5 kcal/mol, respectively.[16]

Photoelectron spectra of CH_3SCN and CH_3NCS were first recorded by Neijzen et al.,[17] and a molecular orbital assignment for the outer valence electron distribution for both species was proposed. However, this initial assignment was later revised by Pasinszki et al.[18] based on ab initio quantum chemical calculations, high-resolution HeI spectra, and HeI/HeII band intensity ratios. Moreover, the ionization process of CH_3SCN and CH_3NCS upon collision with metastable He*(2^3S) has been studied by collision-energy-resolved Penning ionization electron spectroscopy.[19]

Of particular interest for the present work, Hitchcock et al.[20] reported optical oscillator strengths for C 1s, N 1s, and S 2p inner shell excitations in CH_3SCN as derived from electron energy loss spectra. The S 2p region of the spectrum shows the presence of very structured transitions below the ionization potential. These sharp structures have largely been explained in terms of excitations from S 2p electrons to vacant π^* and σ^*_{CS} orbitals.

Our research group has quite recently started studying the properties of shallow and inner core level electrons in sulfenylcarbonyl compounds. Penta-atomic FC(O)SCl[21,22] and ClC(O)SCl[23] species have been studied using synchrotron radiation in the 100−1000 eV range, and their ionic fragmentation after electronic decay has been analyzed. We also studied other members of this family such as $CH_3C(O)SH$[24] and $CH_3OC(O)SCl$.[25] Most recently, we succeeded in analyzing the electronic structure and ionic dissociation induced by photon absorption in the outermost valence region of sulfur-containing species. This study used a combined experimental approach that includes HeI photoelectron spectroscopy and photoionization under the action of synchrotron radiation in the 10−22.5 eV region.[26−28]

Following these studies, we became interested in another simple sulfur-containing compound which presents the advantage of possessing earlier related studies using the inner-shell

* To whom correspondence should be addressed. E-mail: carlosdv@quimica.unlp.edu.ar.
† Universidad Nacional de La Plata.
‡ Laboratorio de Servicios a la Industria y al Sistema Científico.

10.1021/jp807230s CCC: $40.75 © 2009 American Chemical Society
Published on Web 12/22/2008

electron energy loss spectrum (ISEELS) technique. Here we report a study of the photon impact excitation and dissociation dynamics of CH_3SCN exited at the S 2p level using synchrotron radiation. To our knowledge, the inner shell electronic properties and ionic fragmentation of photon-excited CH_3SCN have not been previously described.

Experimental Section

Hazards: *Methyl thiocyanate is a moderately toxic liquid. When heated to decomposition or in contact with mineral acids it emits highly toxic fumes.*

Synchrotron radiation was used at the Laboratório Nacional de Luz Síncrotron (LNLS), Campinas, São Paulo, Brazil.[29] Linearly polarized light monochromatized by a toroidal grating monochromator (available at the TGM beam line in the range 12−300 eV)[30] intersects the effusive gaseous sample inside a high-vacuum chamber with a base pressure in the range of 10^{-8} mbar. During the experiments the pressure was maintained below 5×10^{-6} mbar. The resolution power is better than 400 in the TGM beam-line at the LNLS. The energy calibration was established by means of the S 2p → $6a_{1g}$ and S 2p → $2t_{2g}$ absorption resonances in SF_6.[31] The intensity of the emergent beam was recorded with a light-sensitive diode. The ions produced by interaction of the gaseous sample with the light beam were detected using a time-of-flight (TOF) mass spectrometer of the Wiley−McLaren type for both PEPICO and PEPIPICO measurements.[32,33] This instrument was constructed at the Institute of Physics, Brasilia University, Brasilia, Brazil.[34] The axis of the TOF spectrometer was perpendicular to the photon beam and parallel to the plane of the storage ring. Electrons were accelerated to a multichannel plate (MCP) and recorded without energy analysis. This event starts the flight time determination process of the corresponding ion, which is consequently accelerated to another MCP. The characteristics and performance of this electron-ion coincidence TOF spectrometer have been recently reported.[35]

The average kinetic-energy release (KER) values of the fragments were calculated from the coincidence spectra by assuming an isotropic distribution of the fragments, that they are perfectly space focused, and that the electric field applied in the extraction region is uniform.[36] Under these conditions the energy released in the fragmentation process can be determined from the peak width (fwhm).[37,38] Deviations from ideal conditions always increase the peak width; thus, the values calculated are upper bounds. Santos et al.[39] measured the argon mass spectrum under very similar experimental conditions, and a peak width value of 0.05 eV was achieved for the Ar^+ ion. Because the broadening in argon can only be the result of thermal energy and instrumental broadening, this value represents a good estimation for the instrumental resolution. Moreover, KER values have been determined from the projection of the PEPIPICO islands in the corresponding time domain for each ion involved in the coincidence. The sum of these individual KER values is reported in this work and gives an estimate for the energy release occurring in the double ion dissociation process.

The sample of CH_3SCN was obtained from commercial sources (Aldrich, estimated purity better than 97%). The liquid sample was purified by repeated trap-to-trap vacuum distillation. The purity of the compound in both vapor and liquid phases was checked by IR and ^1H NMR spectroscopies, respectively.

Results and Discussion

The orbital assignment of methyl thiocyanate can be briefly described as follows. The CH_3SCN molecule in the ground electronic state (X^1A_1) belongs to the C_S symmetry point group. All canonical molecular orbitals of type a′ are σ orbitals lying in the molecular plane, while those of type a″ are π orbitals. The 38 electrons are then arranged in 19 doubly occupied orbitals in the independent particle description and distributed according to the following configuration: Core electrons, $[S\ 1s]^2[N\ 1s]^2[C\ 1s]^4[S\ 2s]^2[S\ 2p]^6$; Valence electrons, $(a')^2(a')^2(a')^2(a')^2(a'')^2(a')^2(a')^2(a')^2(a'')^2(a')^2(a'')^2$.

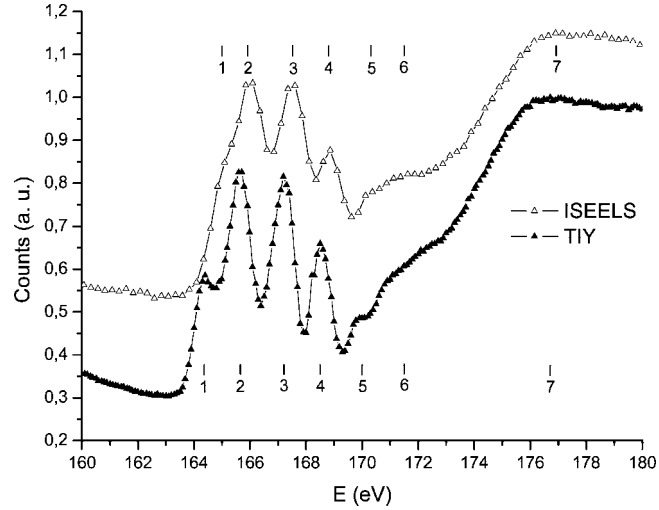

Figure 1. Total ion yield spectrum (▲) and oscillator strengths derived from dipole-regime electron energy loss spectroscopy[20] (Δ) for CH_3SCN. The ISEELS curve is shifted by 0.2 au.

The HOMO can be visualized as an orbital having a″ symmetry, nominally localized on the sulfur atom occupied by lone-pair electrons. Its vertical ionization potential value is 10.13 eV.[17] The HOMO−1 and HOMO−2 orbitals are assigned to both π_{SCN} orbitals of the thiocyanate group. The simple models describe the thiocyanate moiety with a formal triple bond in the C≡N bond, i.e., −S−C≡N. Thus, two different bonds with π symmetry are expected. The bent C−S−C geometry of CH_3SCN removes the degeneracy of both π C≡N molecular orbitals, which are classified as a′ (π_{SCN}) and a″ (π_{SCN}) molecular orbitals. The following two occupied orbitals are assigned to predominantly nonbonding a′ orbitals, occupied by lone pairs nominally belonging to sulfur and nitrogen atoms, respectively.[18]

Total Ion Yield Spectra (TIY). Neither the calculated nor the experimental photoabsorption spectrum for CH_3SCN in the sulfur 2p edge energy region has been reported so far in the literature. The TIY spectra were obtained by recording the count rates of the total ions while the photon energy is scanned. At high photon energies corresponding to shallow− and core−shell electronic levels the quantum yield for molecular ionization is quite likely tending to unity. Consequently, detection of the parent and fragment ions as a function of the incident photon energy is a powerful method to be used as a complement to absorption spectroscopy.[40]

The TIY spectrum of CH_3SCN, measured near the S 2p edge, is shown in Figure 1. Below the S 2p threshold the spectrum is dominated by a group of well-defined signals centered at 164.4, 165.7, 167.2, 168.5, and 170.0 eV. These resonant transitions should correspond to dipole-allowed transitions that involve excitations of a 2p electron to an antibonding molecular orbital. The TIY spectrum of CH_3SCN is remarkably similar to the inner-shell electron energy loss spectrum (ISEELS) reported by Hitchcock et al.[20,41] It is well established that spectra obtained by ISEELS in scattering regimes where electric-dipole transitions dominate are equivalent to optical X-ray absorption

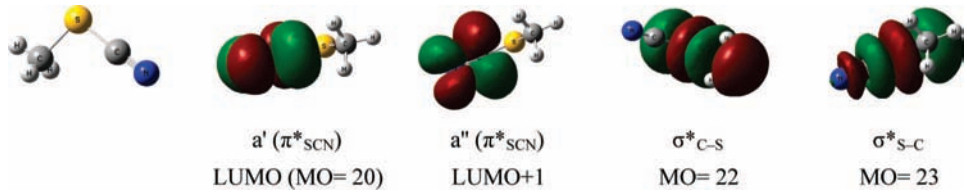

Figure 2. Optimized molecular structure and characters of the four lower energy unoccupied molecular orbitals for CH_3SCN calculated at the MP2/6-311++G(3df) level of approximation.

TABLE 1: Transition Energies (eV) and Proposed Assignments for Features in the Photon (TIY) and Eectron (ISEELS) Excited Spectra of CH_3SCN at the S 2p Level

	TIY (this work)	ISEELS[20]	proposed assignment[20]
1	164.4	165.0 sh	$a'\pi^*_{SCN}$ ($2p_{3/2}$)
2	165.7	165.9	$a''\pi^*_{SCN}$ ($2p_{3/2}$) + $a'\pi^*_{SCN}$ ($2p_{1/2}$)
3	167.2	167.5	σ^*_{CS} ($2p_{3/2}$) + $a''\pi^*_{SCN}$ ($2p_{1/2}$)
4	168.5	168.7	σ^*_{CS} ($2p_{1/2}$)
5	170.0	170.3 sh	Ryd/continuum onset ($2p_{3/2}$)
6	171.5 sh	171.5 sh	Ryd/continuum onset ($2p_{1/2}$)
7	176.7	176.9	2p continuum delayed maximum ($2p_{3/2}$)

spectra.[42] As observed in Figure 1, intense and well-defined pre-edge features are present in both TIY and ISEELS spectra of CH_3SCN. The better resolution obtained in the present case allows clearly identifying two weak transitions at 164.4 and 170.0 eV, reported as shoulders in the former ISEELS spectrum.

Following the proposed assignment for S 2p transitions for CH_3SCN[20] the main features in ISEELS spectra have been assigned to states associated with (S2p, π^*_{SCN}) and (S2p, σ^*_{CS}) configurations. According to the angular momentum selection rules, the final state should have mainly either d or s character. Therefore, the L-edge spectra probe the sulfur d-orbital contributions to the molecular orbitals, which are sensitive to the more distant environment around the sulfur atom.[43,44]

The well-resolved structures observed in the ISEELS and TIY spectra can be interpreted as originated by electronic transitions involving the spin−orbit split of the 2p sulfur excited species ($2p_{1/2}$ and $2p_{3/2}$ levels) to unoccupied antibonding orbitals, mainly the LUMO π^*_{SCN} (a′ and a″) and σ^*_{C-S} orbitals. Quantum chemical calculations at the MP2/6-311++G(3df) level of approximation for neutral CH_3SCN in its ground state predict an unoccupied orbital arrangement which is in agreement with this description (see Figure 2). It is worth mentioning that the σ^*_{S-C} (a′) antibonding MO in the thiocyanate group is slightly higher in energy than the corresponding σ^*_{C-S} (a′) antibonding one assigned to the H_3C-S bond. These results are summarized in Table 1.

This description is in perfect agreement with the assignment of the ISEELS spectra at the S 2p edge proposed by Hitchcock et al.[20] These results are supported by experimental electron transmission and electronic absorption spectra, which allow a description of the vacant orbital of CH_3SCN. Thus, the LUMO corresponds to an antibonding π^*_{SCN} orbital. It was found that both the a′ (π^*_{SCN}) component lying in the C−S−C plane and the perpendicular a″(π^*_{SCN}) component are stabilized by interactions with S(3d) orbitals of appropriate symmetry. The σ^*_{C-S} virtual molecular orbital (LUMO+2) associated with the H_3C-S group is observed in the electron transmission spectra at relatively low energies, in agreement with similar reports observed for other sulfur-containing species.[45] A considerable stabilization of the empty MO's through mixing with the S(3d) and σ^*_{C-S} orbitals was postulated for CH_3SCN.[20]

PEPICO Spectra. PEPICO spectra have been recorded by setting the photon energy at the resonant values observed in the TIY spectrum. In order to identify the role of resonant processes in the fragmentation the spectra were also measured at photon energy values below (typically 10 eV) and above (typically 50 eV) the ionization edge. The PEPICO spectra near the S 2p edge of CH_3SCN are shown in Figure 3.

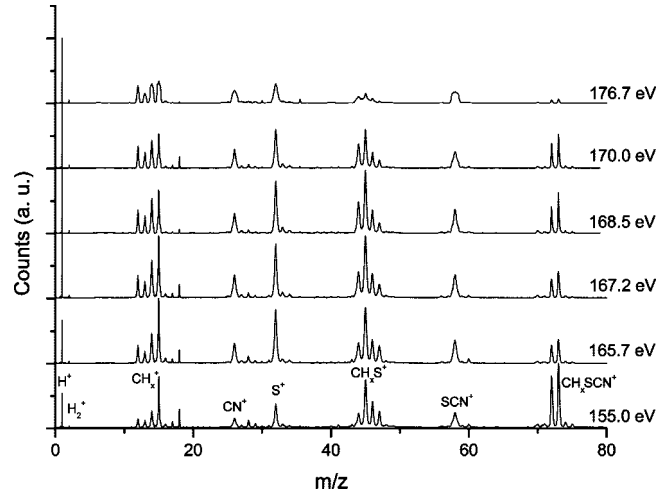

Figure 3. PEPICO spectra of CH_3SCN at selected energies near the S 2p edge.

TABLE 2: Branching Ratios (%) for Fragment Ions Extracted from PEPICO Spectra Taken at Photon Energies around the S 2p Edge for CH_3SCN[a]

		photon energy (eV)					
m/z	ion	155.0	165.7	167.2	168.5	170.0	176.7
1	H^+	5.6/*2.94*	4.9	7.0	8.0	9.5	13.4/*4.86*
2	H_2^+	2.2/*2.43*	0.4	0.7	0.7	1.0	1.6/*5.07*
12	C^+	3.1/*0.72*	4.1	4.8	5.1	5.8	7.0/*2.00*
13	CH^+	2.7/*0.56*	2.8	3.7	4.1	4.7	5.1/*2.88*
14	CH_2^+/N^+	4.9/*0.62*	7.1	8.4	8.2	8.3	11.0/*3.36*
15	CH_3^+	8.9/*0.14*	11.0	10.2	8.0	8.5	12.2/*3.36*
16	S^{2+}	1.7/*0.37*	1.6	1.3	0.6	0.9	1.4/*1.21*
26	CN^+	3.7/*0.45*	5.6	6.2	6.1	6.2	7.8/*2.08*
32	S^+	6.1/*0.23*	11.9	10.6	12.0	11.3	9.4/*0.83*
44	CS^+	3.7/*0.14*	4.8	5.5	6.6	6.0	2.9/*0.35*
45	HCS^+	9.2/*0.11*	10.4	10.6	11.8	8.4	4.1/*0.59*
46	CH_2S^+	4.8/*0.08*	4.4	4.2	4.2	3.3	1.6/*0.29*
47	CH_3S^+	3.3/*0.06*	3.4	2.7	2.0	1.7	0.6/*0.25*
57	$CHSC^+$	0.5/*0.07*	0.3	0.4	0.4	0.4	0.2/*0.22*
58	SCN^+/CH_2SC^+	4.6/*0.20*	5.4	5.1	6.0	5.7	6.4/*0.81*
59	CH_3SC^+	0.6/*0.08*	0.3	0.4	0.4	0.5	0.3/*0.15*
70	$CSCN^+$	1.1/*0.06*	0.4	0.6	0.5	0.5	0.4/*0.18*
71	$CHSCN^+$	1.1/*0.05*	0.4	0.5	0.3	0.3	0.2/*0.17*
72	CH_2SCN^+	6.2/*0.05*	2.0	2.0	2.3	2.6	0.6/*0.16*
73	CH_3SCN^+	7.5/*0.05*	2.5	2.6	3.0	3.2	0.6/*0.15*

[a] Kinetic energy release values determined from the spectra at 155.0 and 176.7 eV are given in italics.

The 70 eV electron impact mass spectrum of CH_3SCN is available in the Web[46] and can serve for comparison with our results. As a whole, the photon impact PEPICO spectra obtained at photon energies around the sulfur 2p threshold resemble the

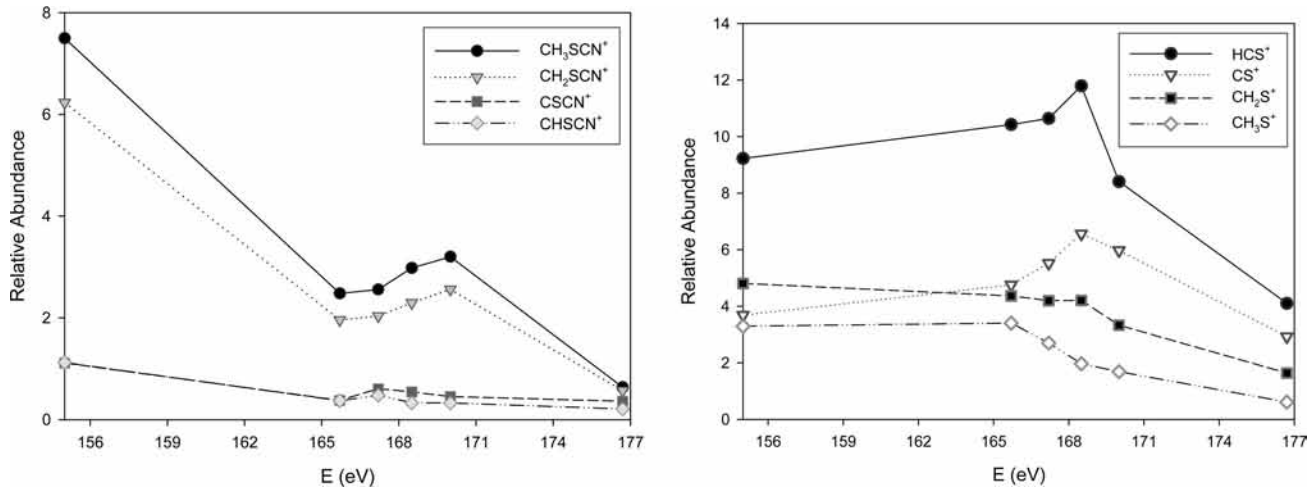

Figure 4. Partial ion yield (PIY) for selected series of ions following photon excitation of CH_3SCN as a function of photon energy.

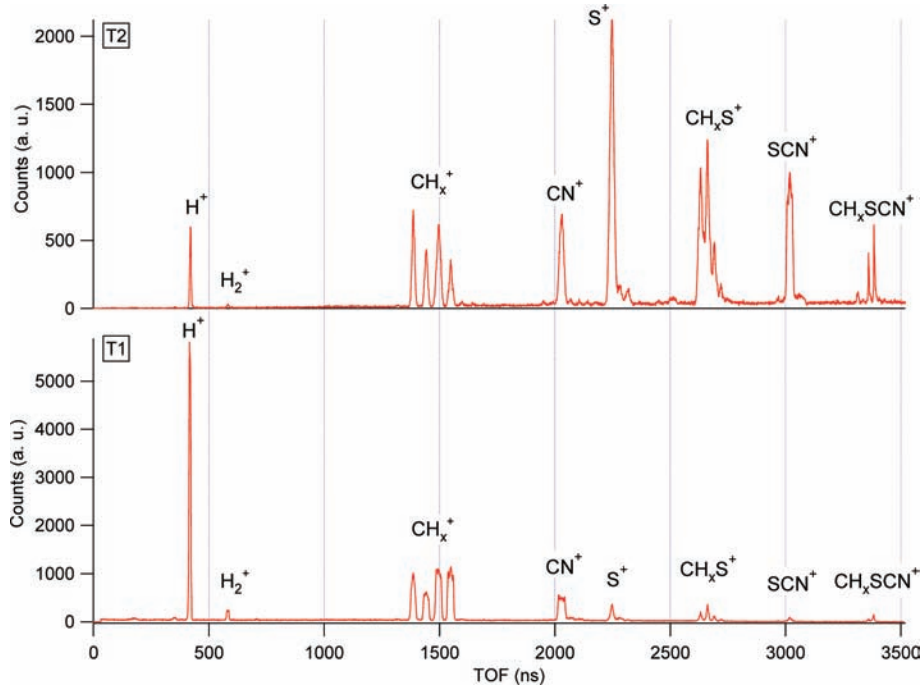

Figure 5. t_1 and t_2 projections of the PEPIPICO spectrum of CH_3SCN recorded at 168.5 eV on the S 2p pre-edge resonance.

electron impact mass spectrum. The parent molecular ion is predominantly formed together with CH_3^+ and HCS^+ fragments. Other ions, such as SCN^+ and S^+, are also observed, showing weaker signals in the spectrum. For instance, in the 155.0 eV spectrum the molecular ion signal at $m/z = 73$ dominates the mass spectra. The more intense peaks observed in the PEPICO spectra correspond to the S^+, CH_3^+, and HCS^+ ions with relative abundances of 6.1%, 8.9%, and 9.2%, respectively. The H^+ ion is also present with an intensity of 5.6%. The next most abundant fragments derive from the SCN group: CN^+ ($m/z = 26$), SCN^+ ($m/z = 58$), and CS^+ ($m/z = 44$) with relative abundances near 4%. The CH_xSCN^+, CH_xSC^+, CH_xS^+, and CH_x^+ ($x = 3-0$) series are also observed. The branching ratios determined from the PEPICO spectra of CH_3SCN at photon energies around the S 2p edge are shown in Table 2.

The kinetic-energy release values have been determined for each ion. In Table 2 the values obtained for two photon energies, i.e., 155.0 and 176.7 eV in the valence and S 2p continuum, respectively, are given. In the former spectrum the ions show KER values which are relatively low, while in the 176.7 eV spectrum a broadening in their peak widths is clearly observed, and all ions show higher KER values. This effect becomes apparent in the PEPICO spectra shown in Figure 3. Therefore, it is possible to assume that the main contribution to the PEPICO spectra below the S 2p threshold comes from fragmentation of single charged parent ion, which is formed by the one-photon ionization process of valence electrons. On the other hand, when the incident photon energy is increased, S 2p electronic excitation or ionization processes occur. It is well known that the decay of such an excited species normally leads to formation of the doubly charged CH_3SCN^{2+} parent ion, for instance, if normal Auger processes take place. This fact is reflected in the KER values for the ions formed at 176.7 eV, which are much broader than the KER values determined for the previous energies.[36]

Dynamics of Fragmentation Following Valence-Shell Ionizations. The estimated double-ionization energy of CH_3SCN is 26.8 eV, as calculated at the MP2/6-311++G** level of approximation. Consequently, 155.0 eV photons should be adequate to open most of the possible ionization channels

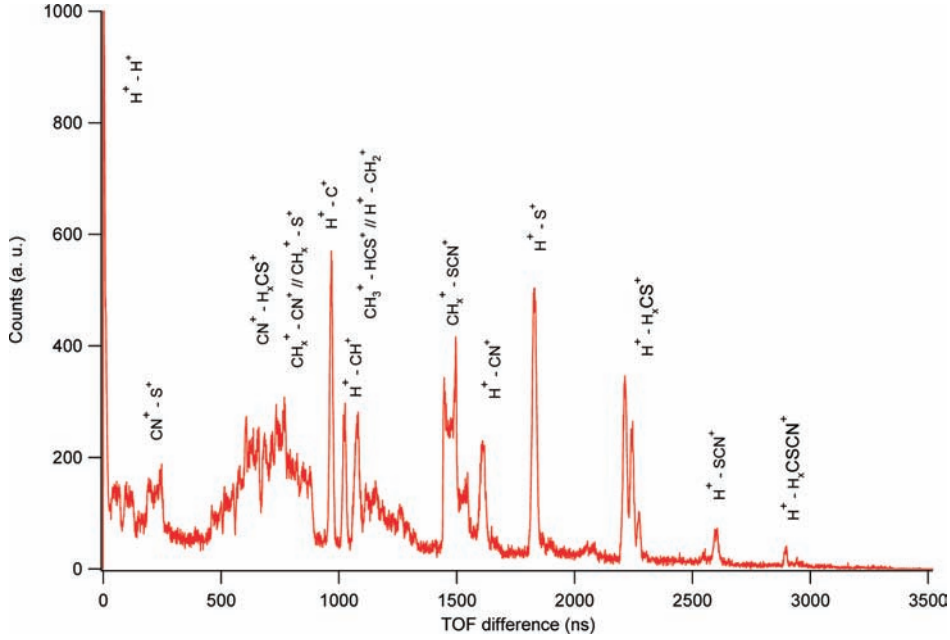

Figure 6. PIPICO projection spectrum of CH_3SCN recorded at 168.5 eV on the S 2p pre-edge resonance.

TABLE 3: Relative Intensities for Double-Coincidence Islands Derived from the PEPIPICO Spectra of CH_3SCN as a Function of the Photon Energy[a]

		photon energy (eV)					
ion 1	ion 2	155.0	165.7	167.2	168.5	170.0	176.7
H^+	C^+	3.7	4.8	6.3	5.4	6.8	7.2
H^+	CH^+	2.0	2.5	3.2	2.7	3.3	3.8
H^+	CH_2^+/N^+	2.8	3.6	4.1	3.3	4.3	5.6
H^+	CN^+	2.4	2.8	3.8	3.3	3.8	4.0
H^+	S^+	4.9	6.3	7.2	7.7	8.6	6.5
H^+	CS^+	3.8	3.8	4.7	4.7	5.1	2.9
H^+	HCS^+	3.8	3.0	3.6	3.4	3.7	2.6
C^+	CH_2^+/N^+	1.4	2.2	2.3	1.9	2.0	2.9
C^+	S^+	2.1	4.3	3.4	3.7	3.8	3.0
CH^+	CN^+			1.2	1.3	1.3	1.3
CH^+	S^+	2.4	3.0	3.2	3.8	3.9	2.6
N^+	CH_3^+		1.5	1.1			
CH_2^+	CN^+	1.4	2.0	2.1	2.0	1.7	2.2
CH_2^+/N^+	S^+	5.4	7.7	7.2	7.0	7.0	5.6
CH_2^+/N^+	SC^+	1.6	2.3	2.2	2.4	2.2	1.5
CH_2^+/N^+	SCN^+/CH_2SC^+	3.8	2.6	2.9	3.3	3.6	3.1
CH_3^+	CN^+	1.1	2.9	1.9	1.3	1.0	1.9
CH_3^+	S^+	4.9	8.8	6.3	4.6	5.0	4.6
CH_3^+	SCN^+	14.1	9.3	9.3	9.8	12.9	10.0
CN^+	S^+	1.6	3.1	2.8	2.9	2.4	2.7
CN^+	CS^+	1.1		1.1	1.4	1.2	
CN^+	HCS^+	4.7	4.7	4.3	4.2	3.5	2.3

[a] Only coincidences with intensities > 1% are given.

connected to the direct single and double ejections of valence-shell electrons. As observed in the TIY spectra, this energy is not yet enough to ionize the core electrons. Thus, the coincidence spectrum taken at a 155.0 eV photon energy should provide a good comparison with respect to the ionic fragmentation pattern associated with core excitation or ionization.

The single charged molecular ion is observed in the whole range of photon energies studied. A clear diminution of the peak intensity for CH_3SCN^+ ion is observed when resonant energies are reached with typical abundance values of around 3%. When S 2p electrons are ionized, further diminution in the CH_3SCN^+ ion signal intensity becomes apparent, as observed in the PEPICO spectrum taken at 176.7 eV. The KER values determined for this ion are close to the "thermal" value of 0.05 eV.[39]

The CH_xSCN^+ series of ions can be unambiguously characterized as formed from the parent ion by successive loss of hydrogen atoms. The KER values, ca. 0.05 eV, are very similar to those determined for the CH_3SCN^+ ion. Indeed, it is expected that extrusion of a neutral hydrogen atom from charged CH_xSCN^+ ($x = 3, 2, 1$) has a little impact in the KER of the remaining ions. The partial ion yield spectra for the series of CH_xSCN^+ ($x = 3-0$) ions near the S 2p edge are displayed in Figure 4. When CH_3SCN is irradiated with 155.0 eV photons in the valence continuum region of the spectrum, CH_xSCN^+ ($x = 3-0$) ions are responsible for ca. 16% of single ionization.

On the other hand, processes that yield charged hydrogen atoms (H^+) are evident from the intense signal at $m/z = 1$ amu/q. Although an unambiguous description of these processes is not possible at this point, it should be noted that the high KER value determined for the H^+ ion could denote ejection of an energetic ion. Similarly, high KER values are determined for the H_2^+ ion, which is a typical signature of processes involving rearrangement reactions.[47] It should be mentioned that studies on the decomposition of electronically excited CH_3SCN have concluded that the main primary dissociation step forming SCN involves a rearrangement reaction to afford H_2 ($CH_3SCN \rightarrow CH + H_2 + SCN$).[48]

Rupture of both sulfur−carbon bonds in single charged CH_3SCN^+ can also be observed. First, the H_3C-S bond can easily be broken to yield both the CH_3^+ or SCN^+ ions. Again, in the former case successive losses of hydrogen atoms lead to the observation of the series of CH_x^+ ($x = 3-0$) ions. From the determined KER values, the following mechanisms can be proposed

$$CH_3SCN^+ \rightarrow CH_3^+ + SCN \quad (KER \approx 0.14\ eV)$$

$$CH_3SCN^+ \rightarrow CH_3 + SCN^+ \quad (KER \approx 0.20\ eV)$$

Moreover, it is quite interesting to note that fragments such as CH_xS^+ ($x = 3-0$) or CN^+ are also present in the PEPICO spectra depicted in Figure 3. These ions are associated with rupture of the carbon−sulfur bond in the thiocyanate group. Indeed, the series of CH_xS^+ ($x = 3-0$) ions accounts for the ca. 21% of ions detected in the 155.0 eV spectrum. The PIY

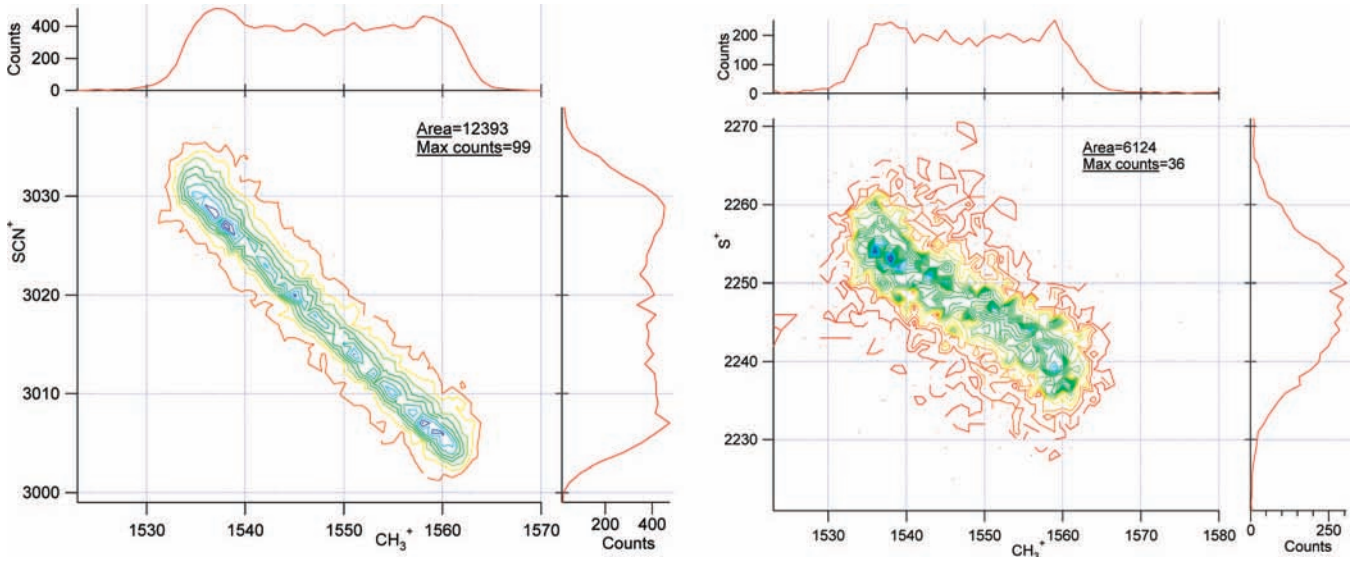

Figure 7. Contour plot for the coincidence island between CH_3^+ and SCN^+ ions (left) and between CH_3^+ and S^+ ions (right) derived from the 168.5 eV PEPIPICO spectrum.

spectra for these ions are shown in Figure 4. When resonant energies are reached an increment in the production of HCS^+ and CS^+ ion signals is observed with a maximum at 168.5 eV. Electronic transitions that populate the σ^*_{S-C} antibonding orbital could take place. The most abundant ion of this series corresponds to the HCS^+ ion, which is known to possess a high thermodynamic stability.[49,50] The KER values determined for these ions are relatively low, denoting a minor impact in the kinetic-energy release when a neutral hydrogen atom is extruded from the fragment. The following consecutive dissociation channels are proposed

$$CH_3SCN^+ \rightarrow CH_3S^+ + CN \quad (KER \approx 0.06\ eV)$$

$$CH_3S^+ \rightarrow CH_2S^+ + H \quad (KER \approx 0.08\ eV)$$

$$CH_2S^+ \rightarrow HCS^+ + H \quad (KER \approx 0.11\ eV)$$

As mentioned before, a common feature of the single charged ions is an impressive peak broadening observed on moving from 155.0 to 176.7 eV through S 2p excitation, denoting the importance of Auger-induced double-ionization and fragmentation processes. Thus, multicoincidence spectra allowing for detection of at least two ions are required in order to analyze the dynamic of fragmentation of sulfur excited CH_3SCN.

PEPIPICO Spectra. Two-dimensional PEPIPICO spectra for the correlation between one electron and two positive ions were recorded at each of the resonant energy values in the S 2p region. Projections of PEPIPICO spectra of CH_3SCN on the t_1 and t_2 axes were obtained by integrating the signal intensities over the corresponding time domains. These projections for the spectrum recorded at 168.5 eV are depicted in Figure 5. The H^+ ion signal strongly dominates the t_1 domain followed in importance by the CH_x^+ ($x = 3-0$) group of ions at TOF around 1500 ns and those related to m/z values of 26 (CN^+) and 32 (S^+) amu/q. A very weak signal observed for the M^+ ion in the t_1 domain at 3400 ns can be associated with false coincidences.

The t_2 projection is dominated by the ion signal centered at 2200 ns, corresponding to the m/z ion ratio of 32 amu/q, while other signals with significant intensities are those related to CH_x^+ ($x = 3-0$), CN^+, H_xCS^+ (3−0), and SCN^+ ions. Identification of the CH_x^+ ($x = 2-0$) group of ions in the t_2 domain implies that H^+ is formed as the lighter ion (appearing in the t_1 domain). Judging from the presence of the CH_3^+ peak in the t_2-projected spectrum, coincidences with C^+ or N^+ ions from the SCN group are expected. The heaviest fragment observed in the t_2 domain is the M − 1 ion, CH_2SCN^+. The signal appearing at times corresponding to the H^+ ion in the t_2 domain is associated with H^+-H^+ double coincidence, although the limited multihit resolution and possible discrimination effects against light ions could affect this signal.

The PIPICO projections for the TOF difference (t_2 minus t_1) domain were also analyzed. Figure 6 shows the spectrum recorded at 168.5 eV on the S 2p resonance including an assignment of the main peaks. A strong signal is evident for TOF differences close to 0 related with H^+/H^+ double coincidence. As suggested from the previous analysis of the PEPIPICO projection, the progression of coincidences involving the H^+ ion as the lighter fragment is clearly observed. Thus, H^+/CH_x^+ ($x = 2-0$), H^+/CN^+, H^+/S^+, H^+/SCN^+, and H^+/CH_xSCN^+ ($x = 2-0$) double coincidences are easily identified as well-defined signals. A broad unresolved signal is also observed at TOF differences between 500 and 800 ns, encompassing the CN^+/CH_xS^+, CH_x^+/CN^+, and CH_x^+/S^+ ($x = 3-0$) double coincidences. The CH_x^+/SCN^+ gives rise to a clear defined signal at a TOF difference of 1480 ns.

Dynamics of Fragmentation for the CH_3SCN^{2+} Ion. It is well known that core excitation and core ionization lead to resonant and normal Auger processes, which are highly effective electronic decay mechanisms in promoting dissociation of molecules. Analysis of the PEPIPICO spectra is useful for identifying two-, three-,[32] and four-body dissociation mechanisms which follow Auger decay mechanisms.[51,52] As a first approximation, in the analysis of the PEPIPICO spectra the following two aspects were taken into account. First, due to the inherent limited resolution used in the experiments, for islands involving m/z values of 14 amu/q, the distinction between N^+ and CH_2^+ ions is not always possible. Second, the peaks corresponding to double coincidences involving m/z values of 1, 12, 14, and 32 amu/q are the most intense signals, reflecting the importance of the atomization processes in the dissociation mechanisms of CH_3SCN. These processes may be originated by several multibody dissociation events that reduce to the same

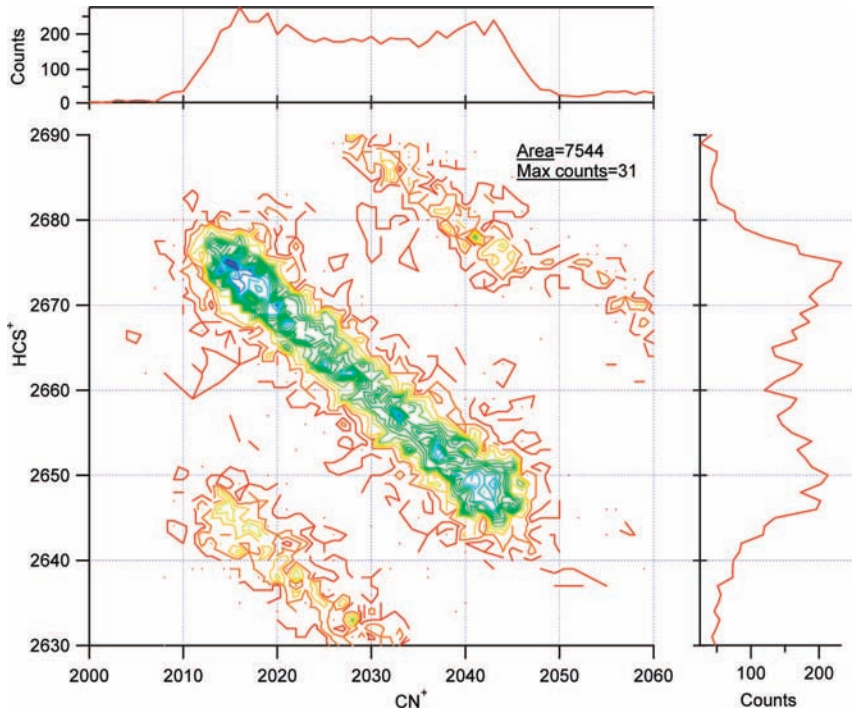

Figure 8. Contour plot for the coincidence island between CN^+ and HCS^+ ions derived from the 168.5 eV PEPIPICO spectrum.

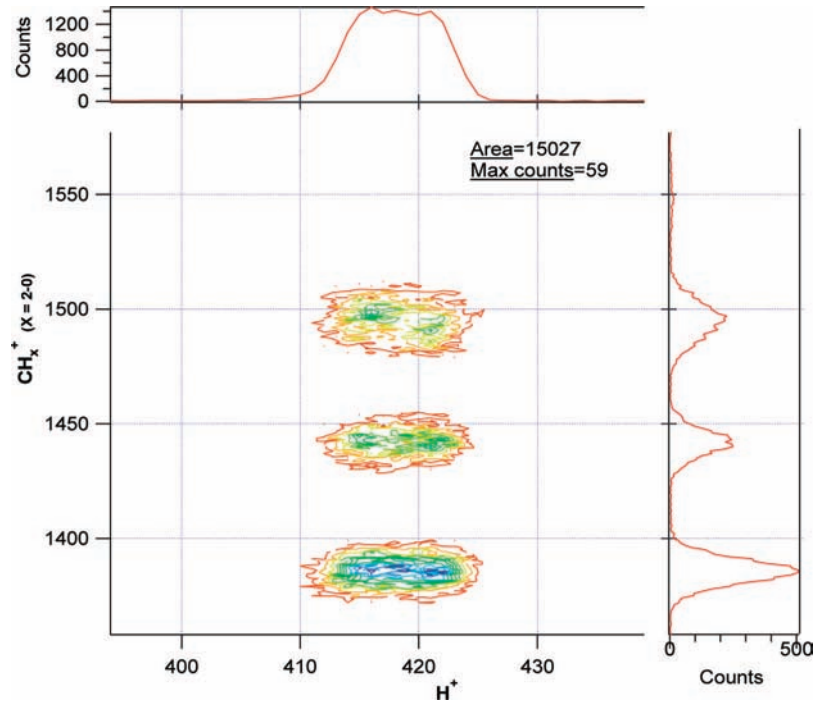

Figure 9. Contour plot for the coincidence island between H^+ and CH_x^+ ($x = 0-2$) ions derived from 168.5 eV PEPIPICO spectrum.

final pair of atomic ions, making analysis of these coincidences ambiguous. Taking into consideration these facts, attention is paid to selected pairs of ions for which both good statistics and well-defined shapes are observed. In particular, ionic fragments originated by ruptures in the thiocyanate moiety will be considered.

The double coincidence branching ratios and KER values for double ion processes calculated from PEPIPICO spectra at several photon energies are given in Table 3. The experimental slopes for coincidence islands were determined at both resonance and off-resonance photon energies in the S 2p region, and no significant changes in the dissociation mechanism were observed. The following discussion will refer to slopes determined from the PEPIPICO spectrum taken at a 168.5 eV photon energy.

Fragmentation processes leading to formation of CH_3^+ and SCN^+ ions dominate the dissociation of CH_3SCN excited at the S 2p levels. The parallelogram-like shape of the island and the observed slope close to -1.0 (Figure 7) can be explained by a two-body mechanism

$$CH_3SCN^{+2} \rightarrow CH_3^+ + SCN^+ \quad (KER = 5.6\ eV)$$

This coincidence represents the most intense island in the 155.0 eV PEPIPICO spectrum with a relative abundance of 14.1%. This value decreases when the photon energy reaches the resonant transition values. A concomitant increment in the CH_3^+/S^+ double coincidence intensity is observed. For this island (Figure 7) the experimental slope (near −0.6) can be explained by a secondary decay mechanism[52]

$$\begin{aligned} CH_3SCN^{2+} &\rightarrow CH_3^+ + SCN^+ \\ SCN^+ &\rightarrow CN + S^+ \end{aligned} \quad KER = 4.7\ eV$$

In this case, the SCN^+ ion formed in the first step undergoes a second dissociation process to give S^+. Both two- and three-body mechanisms seem to be coupled, as shown in the following scheme.

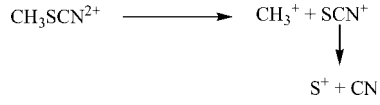

For the CN^+/S^+ pair of ions a medium intensity coincidence with a branching ratio of 3.1% at 165.7 eV is observed with a −0.7 slope. In principle, several dissociation channels can be proposed to explain this coincidence. However, the occurrence of a typical deferred charge separation or a concerted fragmentation mechanism must be discarded because both fragmentations would imply a coincidence with a slope of −1.0 independent of the relative masses of the fragments. For example, in a deferred charge separation scheme for CH_3SCN the C−S bond is broken in a first step, the charge being retained in the SCN fragment, and dissociation of the dication taking place in the second step

$$CH_3SCN^{2+} \rightarrow CH_3 + SCN^{2+}$$

$$SCN^{2+} \rightarrow CN^+ + S^+$$

Thus, the coincidence observed for CN^+/S^+ ions must involve the early rupture of the S−C bond of the −SCN group. A three-body secondary decay mechanism is proposed

$$\begin{aligned} CH_3SCN^{2+} &\rightarrow CH_3S^+ + CN^+ \\ CH_3S^+ &\rightarrow CH_3 + S^+ \end{aligned} \quad KER = 6.2\ eV$$

The calculated slope of −0.68 is in good agreement with the experimental value of −0.7 derived from the PEPIPICO spectra.

The coincidence between CN^+ and HCS^+ ions can be originated in a four-body secondary decay involving the same very first step as the previous mechanisms followed by the loss of neutral hydrogen atoms. The calculated slope for this mechanism is −0.96, in very good agreement with the experimental value of −1.0, as shown in Figure 8.

$$\begin{aligned} CH_3SCN^{2+} &\rightarrow CH_3S^+ + CN^+ \\ CH_3S^+ &\rightarrow CH_2S^+ + H \\ CH_2S^+ &\rightarrow HCS^+ + H \end{aligned} \quad KER = 4.7\ eV$$

Rupture of the S−C bond of the thiocyanate group to yield CN^+ ions is responsible for ca. 8% of the fragmentation channels followed by CH_3SCN^{2+}. These dissociation pathways originating in rupture of the S−CN bond can be qualitatively sketched taking the mutual dependency of the double coincidence intensities for the corresponding ion islands into account (Table 3).

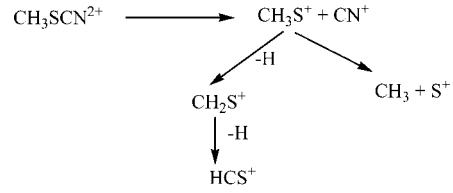

The high stability of the HCS^+[49,50] precludes subsequent dissociation of this ion. Thus, the CN^+/CS^+ coincidence is observed as a very low intensity signal (∼1%) in the PEPIPICO spectra.

Finally, the double coincidences involving H^+ and the CH_x^+ ($x = 2-0$) group of ions have been analyzed. As anticipated from the projection spectra discussed above, observance of the ions with $m/z = 12$, 13, and 14 requires that H^+ arrives as the lighter ion. Additionally, when the heavier ion has a m/z ratio of 13, the only possibility corresponds to the H^+/CH^+ pair of ions for CH_3SCN. The contour plot obtained from the PEPIPICO spectrum at 168.5 eV for arrival times corresponding to H^+ and $12 < m/z < 15$ ions is shown in Figure 9. Note that, as expected, the H^+/CH_3^+ coincidence is absent. The three coincidences are parallel with slopes close to zero, suggesting that a secondary decay mechanism occurs

$$CH_3SCN^{2+} \rightarrow CH_2SCN^+ + H^+ \quad KER = 8.6\ eV\ (mean\ value)$$

$$CH_2SCN^+ \rightarrow CH_X^+ + SCN + (2-x)H^0 \quad (x = 0-2)$$

The calculated slopes assuming the sequential mechanism are −0.19, −0.18, and −0.17 for the H^+/CH_2^+, H^+/CH^+, and H^+/C^+ double coincidences, respectively.

Conclusions

A detailed study of the ionic fragmentation of the CH_3SCN molecule in the gas phase following continuum valence and S 2p excitations has been performed using multicoincidence techniques based on time-of-flight mass spectrometry and synchrotron radiation as the photon source. The transitions observed in the TIY spectrum near the S 2p edge show an excellent agreement with the optical oscillator strengths derived from electron energy loss spectra recorded under electric dipole-dominated conditions.[20]

The dynamics of the fragmentation of charged hydrocarbon species is strongly dominated by rupture of C−H bonds. As proposed by Montenegro et al.[53] the processes that take place can be characterized either as "evaporation", eliminating light H^0 neutral atoms, or "fission", ejecting H^+ ions, or the molecule can break up into two or more charged fragments. Both evaporation and fission processes are clearly observed in the valence continuum and S 2p excited CH_3SCN. Double coincidences involving production of H^+ as the lighter ion dominate the PEPIPICO spectra, being responsible for at least 30% of the fragmentation of S 2p excited CH_3SCN.

Other dissociation mechanisms were also observed from the analysis of the double coincidence islands. Electronic excitations to the σ^*_{C-S} antibonding molecular orbital should play a key role in the dynamics of many fragmentation process. In particular, the two-body dissociation mechanism yielding CH_3^+ and SCN^+ single charged molecular ions is observed with abundances around 10% of the double coincidences. A similar mechanism that involves rupture of the C−S single bond dominates the dissociation of electronically excited neutral CH_3SCN.[12,13] The virtual σ^*_{S-C} orbital corresponding to the thiocyanate group has received less attention. Our calculations predict that both σ^*_{C-S} and σ^*_{S-C} unoccupied molecular orbitals

should influence the electronic properties of CH_3SCN. Fragmentation of methyl thiocyanate excited at the S 2p edge produces a series of ions arising from rupture of the S−CN bond of the thiocyanate moiety. Thus, the group of double coincidences CN^+/S^+, CN^+/HCS^+, and CN^+/CS^+ accounts for near 8% of the ion signals in the PEPIPICO spectra. This fact represents indirect evidence that supports the significant role of the σ^*_{S-C} MO in the dynamics of fragmentation of CH_3SCN.

It is interesting to note, also, the significant enhancement in the branching ratios for double coincidences involving the S^+ ion at the S 2p excitation energies. The sum of double coincidences having S^+ as the heavier ion is ca. 21% below the S 2p ionization edge. This value increases to 33% of the double coincidence production at the first resonance transition (165.7 eV). This could be an indication that state-specific fragmentation[54,55] occurs in S 2p excited CH_3SCN. These results invite one to perform further studies on selective C 1s and/or N 1s core level photoionization.

Acknowledgment. This work has been largely supported by the Brazilian Synchrotron Light Source (LNLS) under proposal D05A-TGM-6535. The authors wish to thank Arnaldo Naves de Brito and his research group for fruitful discussions and generous collaboration during their several stays in Campinas and the TGM beamline staff for their assistance throughout the experiments. They are indebted to the Agencia Nacional de Promoción Científica y Tecnológica (ANPCyT), Consejo Nacional de Investigaciones Científicas y Técnicas (CONICET), and the Comisión de Investigaciones Científicas de la Provincia de Buenos Aires (CIC), República Argentina, for financial support. We also thank the Facultad de Ciencias Exactas, Universidad Nacional de La Plata, República Argentina, for financial support. C.O.D.V. especially acknowledges the DAAD, which generously sponsors the DAAD Regional Program of Chemistry for the República Argentina supporting Latin-American students to receive their Ph.D. in La Plata. Finally, we thank referee 2 for his/her time and effort in doing such a constructive review. We highly appreciate his/her contributions in improving the content, quality, and presentation of this work. E.C. and M.G. are doctoral fellows of CONICET. M.F.E., C.O.D.V., and R.M.R. are members of the Carrera del Investigador of CONICET.

References and Notes

(1) Mukerjee, A. K.; Ashare, R. *Chem. Rev.* **1991**, *91*, 1.
(2) Erian, A. W.; Sherif, S. M. *Tetrahedron* **1999**, *55*, 7957.
(3) Sharma, S. *J. Sulfur Chem.* **1989**, *8*, 327.
(4) Moore, C. B.; Álvarez, R. A. *Science* **1994**, *263*, 205.
(5) Dreizler, H.; Rudolph, H. D.; Schleser, H. *Z. Naturforsch.* **1970**, *25A*, 1643.
(6) Jonathan, P.; Hamdan, M.; Brenton, A. G.; Willett, G. D. *Chem. Phys.* **1988**, *119*, 159.
(7) Babinec, P.; Leszczynski, J. *J. Mol. Struct. (Theochem)* **2000**, *277*, 501–502.
(8) Fu, Z.; Pan, X.-M.; Li, Z.-S.; Sun, C.-C.; Wang, R.-S. *Chem. Phys. Lett.* **2006**, *430*, 13.
(9) Crowder, G. A. *J. Mol. Spectrosc.* **1967**, *23*, 108.
(10) Maienschein-Cline, M. G.; Londergan, C. H. *J. Phys. Chem. A* **2007**, *111*, 10020.
(11) Li, P.; Ling Tan, Y.; Yip Fan, W. *Chem. Phys.* **2004**, *302*, 171.
(12) Tokue, I.; Hiraya, A.; Shobatake, K. *Chem. Phys.* **1987**, *117*, 315.
(13) Tokue, I.; Kobayashi, K.; Honda, T.; Ito, Y. *J. Phys. Chem.* **1990**, *94*, 3485.
(14) Northrup, F. J.; Sears, T. J. *J. Chem. Phys.* **1990**, *93*, 2337.
(15) Northrup, F. J.; Sears, T. J. *J. Chem. Phys.* **1990**, *93*, 2346.
(16) Karpas, Z.; Stevens, W. J.; Buckley, T. J.; Metz, R. *J. Phys. Chem.* **1985**, *89*, 5274.
(17) Neijzen, B. J. M.; De Lange, C. A. *J. Electron Spectrosc. Relat. Phenom.* **1980**, *18*, 179.
(18) Pasinszki, T.; Veszprèmi, T.; Fehèr, M.; Kovac, B.; Klasinc, L.; Mcglynn, S. P. *Int. J. Quantum Chem., Quantum Chem. Symp.* **1992**, *26*, 443.
(19) Pasinszki, T.; Yamakado, H.; Ohno, K. *J. Phys. Chem.* **1993**, *97*, 12718.
(20) Hitchcock, A. P.; Tronc, M.; Modelli, A. *J. Phys. Chem.* **1989**, *93*, 3068.
(21) Erben, M. F.; Romano, R. M.; Della Védova, C. O. *J. Phys. Chem. A* **2004**, *108*, 3938.
(22) Geronés, M.; Erben, M. F.; Romano, R. M.; Della Védova, C. O. *J. Electron Spectrosc. Relat. Phenom.* **2007**, *155*, 64.
(23) Erben, M. F.; Romano, R. M.; Della Védova, C. O. *J. Phys. Chem. A* **2005**, *109*, 304.
(24) Erben, M. F.; Geronés, M.; Romano, R. M.; Della Védova, C. O. *J. Phys. Chem. A* **2006**, *110*, 875.
(25) Erben, M. F.; Geronés, M.; Romano, R. M.; Della Védova, C. O. *J. Phys. Chem. A* **2007**, *111*, 8062.
(26) Geronés, M.; Erben, M. F.; Romano, R. M.; Della Védova, C. O.; Yao, L.; Ge, M. *J. Phys. Chem. A* **2008**, *112*, 2228.
(27) Erben, M. F.; Della Védova, C. O. *Inorg. Chem.* **2002**, *41*, 3740.
(28) Geronés, M.; Downs, A. J.; Erben, M. F.; Ge, M.; Romano, R. M.; Yao, L.; Della Védova, C. O. *J. Phys. Chem. A* **2008**, *112*, 5947.
(29) Lira, A. C.; Rodrigues, A. R. D.; Rosa, A.; Gonçalves da Silva, C. E. T.; Pardine, C.; Scorzato, C.; Wisnivesky, D.; Rafael, F.; Franco, G. S.; Tosin, G.; Lin, L.; Jahnel, L.; Ferreira, M. J.; Tavares, P. F.; Farias, R. H. A.; Neuenschwander, R. T. First Year Operation of the Brazilian Sinchrotron Light Source. European Particle Accelerator Conference, Stockholm, Sweden, 1998.
(30) de Fonseca, P. T.; Pacheco, J. G.; Samogin, E.; de Castro, A. R. B. *Rev. Sci. Instrum.* **1992**, *63*, 1256.
(31) Kivimaki, A.; Ruiz, J. A.; Erman, P.; Hatherly, P.; Garcia, E. M.; Rachlew, E.; Riu, J. R. i.; Stankiewicz, M. *J. Phys. B: At. Mol. Opt. Phys.* **2003**, 781.
(32) Frasinski, L. J.; Stankiewicz, M.; Randall, K. J.; Hatherly, P. A.; Codling, K. *J. Phys. B: At. Mol. Phys* **1986**, *19*, L819.
(33) Eland, J. H. D.; Wort, F. S.; Royds, R. N. *J. Electron Spectrosc. Relat. Phenom.* **1986**, *41*, 297.
(34) Naves de Brito, A.; Feifel, R.; Mocellin, A.; Machado, A. B.; Sundin, S.; Hjelte, I.; Sorensen, S. L.; Bjorneholm, O. *Chem. Phys. Lett.* **1999**, *309*, 377.
(35) Burmeister, F.; Coutinho, L. H.; Marinho, R. R.; Homem, M. G. P.; de Morais, M. A. A.; Mocellin, A. ; Björneholm, O.; Sorensen, S. L. ; de Fonseca, P. T.; Lindgren, A.; Naves de Brito, A. *J. Electron Spectrosc. Relat. Phenom.* **2008**, in press; doi:10.1016/j.elspec.2006.05.007.
(36) Laskin, J.; Lifshitz, C. *J. Mass Spectrom.* **2001**, *36*, 459.
(37) Hansen, D. L.; Arrasate, M. E.; Cotter, J.; Fisher, G. R.; Hemmers, O.; Leung, K. T.; Levin, J. C.; Martin, R.; Neill, P.; Perera, R. C. C.; Sellin, I. A.; Simon, M.; Uehara, Y.; Vanderford, B.; Whitfield, S. B.; Lindle, D. W. *Phys. Rev. A* **1998**, *58*, 3757–3765.
(38) Simon, M.; LeBrun, T.; Morin, P.; Lavollée, M.; Maréchal, J. L. *Nucl. Instrum. Methods* **1991**, *B62*, 167.
(39) Santos, A. C. F.; Lucas, C. A.; de Souza, G. G. B. *J. Electron Spectrosc. Relat. Phenom.* **2001**, *115*, 114–116.
(40) Nenner, I.; Beswick, J. A. Molecular Photodissociation and Photoionization. In *Handbook on Synchrotron Radiation*; Marr, G. V., Ed.; Elsevier Science Publishers: Amsterdam, 1987; Vol. 2; p 355.
(41) Hitchcock, A. P. http://unicorn.mcmaster.ca/corex/cedb-title.html.
(42) Hitchcock, A. P. *J. Electron Spectrosc. Relat. Phenom.* **1982**, *25*, 245.
(43) Jalilehvand, F. *Chem. Soc. Rev.* **2006**, *35*, 1256.
(44) Hudson, E.; Shirley, D. A.; Domke, M.; Remmers, G.; Puschmann, A.; Mandel, T.; Xue, C.; Kaindl, G. *Phys. Rev. A* **1993**, *47*, 361.
(45) Hitchcock, A. P.; Horsley, J. A.; Stohr, J. *J. Chem. Phys.* **1986**, *85*, 4835.
(46) Stein, S. E. *NIST Mass Spectroscopy Data Center, NIST Standard Reference Database Number 69*; Linstrom, P. J., Mallard, W. G., Eds.; National Institute of Standards and Technology: Gaithersburg, MD, March 2003.
(47) Lago, A. F.; Santos, A. C. F.; de Souza, G. G. B. *J. Chem. Phys.* **2004**, *120*, 9547.
(48) Nicholas, J. E.; Amodio, C. A. *J. Chem. Soc., Faraday Trans. 1* **1980**, *76*, 1669.
(49) Smith, D. *Chem. Rev.* **1992**, *92*, 1473.
(50) Thaddeus, P.; Guélin, M.; Linke, R. A. *Astrophys. J.* **1981**, *246*, L41.
(51) Eland, J. H. D. *Mol. Phys.* **1987**, *61*, 725.
(52) Simon, M.; Lebrun, T.; Martins, R.; de Souza, G. G. B.; Nenner, I.; Lavollee, M.; Morin, P. *J. Phys. Chem.* **1993**, *97*, 5228.
(53) Montenegro, E. C.; Scully, S. W; Wyer, J. A.; Senthil, V.; Shah, M. B. *J. Electron Spectrosc. Relat. Phenom.* **2007**, *155*, 81.
(54) Eberhardt, W.; Sham, T. K.; Carr, R.; Krummacher, S.; Strongin, M.; Weng, S. L.; Wesner, D. *Phys. Rev. Lett.* **1983**, *50*, 1038.
(55) Miron, C.; Simon, M.; Leclercq, N.; Hansen, D. L.; Morin, P. *Phys. Rev. Lett.* **1998**, *81*, 4104.

JP807230S